THE JOURNAL OF PHYSICAL CHEMISTRY C

Article

Cite This: J. Phys. Chem. C 2018, 122, 143−149

pubs.acs.org/JPCC

Well-Dispersed Vanadium Nitride on Porous Carbon Networks Derived from Block Copolymer of PAN-*b*-PDMC-*b*-PAN Absorbed with Ammonium Metavanadate for Energy Storage Application

Ying Liu,[†,‡] Lingyang Liu,[§] Yongtao Tan,[†,‡] Lingbin Kong,[†,‡] Long Kang,[†,‡] and Fen Ran*[,†,‡]

[†]State Key Laboratory of Advanced Processing and Recycling of Non-ferrous Metals, Lanzhou University of Technology, Lanzhou 730050, P. R. China

[‡]School of Material Science and Engineering, Lanzhou University of Technology, Lanzhou 730050, Gansu, P. R. China

[§]Laboratory of Clean Energy Chemistry and Materials, State Key Laboratory of Solid Lubrication, Lanzhou Institute of Chemical Physics, Chinese of Academy of Sciences, Lanzhou 730000, P. R. China

Supporting Information

ABSTRACT: Both vanadium nitride and carbon are the important negative materials for capacitors electrodes, while effectively dispersing vanadium nitride into the surface of carbon materials would highly enhance the utilization of active materials. In this article, we find out a valid dispersion method of vanadium nitride nanoparticles into the porous carbon networks, which is derived from a synthesized block copolymer of polyacrylonitrile-*b*-poly[2-(methacryloyloxy)ethyl]trimethylammonium chloride-*b*-polyacrylonitrile together with the absorbed ammonium metavanadate. With the superiority of the designed structure, the fabricated materials are used as negative materials for capacitors electrodes and show outstanding electrochemical performance with a specific capacitance of 195.7 F/g and a prior cycle stability of 75% retention. In addition, the effect of the ratio of copolymer to ammonium metavanadate on the electrochemical performance of the product is also investigated in detail.

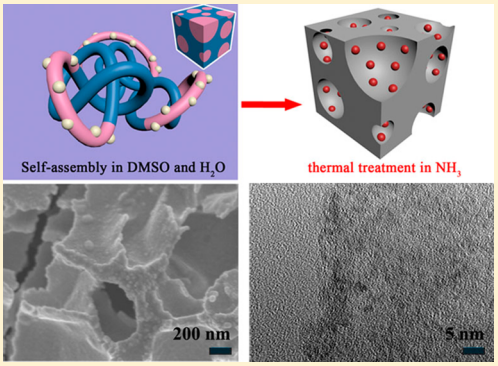

1. INTRODUTION

For the clean renewable energy, both opportunities and challenges come with the gradually exhausted nonrenewable energy resources. It is generally known that most clean renewable energy is unevenly distributed and intermittent. The best way to solve these problems is to transfer the energy into an electric one. This made the electrical energy storage (EES) play a more and more important role in our daily lives.[1−6] EES technologies include capacitors, batteries, and others; however, both of them have limitations. Although a battery has high energy density, but compared to a capacitor, its power density is low. Furthermore, the cycle life, rate performance, and safety of a battery are also barely satisfactory. As a comparison, capacitors show high rate performance, good cycle life, and high power density, although its energy density is still low.[7−15]

As we all know, the energy density of capacitors is highly related to the specific capacitance and the square of voltage window in the electrochemical process. Thus, the most efficient methods to enhance energy density include increasing the ability of charge storage and widening the ultimate work potential.[16−18] The working potential is decided by both electrolyte and electrode materials including positive and negative ones. Considering it in an economic viewpoint, the aqueous electrolyte is still the best choice for the capacitors.[19,20] Thus, enhancing the performance of electrode materials is one of the best ways to overcome the limitation. Up to now, an overwhelming majority of researches for electrode materials focus on positive electrode materials, such as transition-metal oxides, metal sulfide, conducting polymers, and so on.[21−26] The most used negative materials for capacitors are mainly concentrating on carbon materials because of their low weight and low cost, high power density, fast charging/discharging kinetics, long cycle life, and bipolar operational flexibility.[27−31] Nevertheless, the charge storage and work potential of carbon materials as negative electrode are still limited.

As negative materials, transition-metal nitrides are a good choice for capacitors; especially, vanadium nitride (VN) has an impressive specific capacity and large work potential in an aqueous environment.[32,33] Hence, various types of VN nanostructures have been constructed as negative electrodes, such as nanoparticle, nanofiber, and nanotube.[34−36] However, effectively dispersing these vanadium nitrides into the surface of carbon materials is the best method to highly enhance the utilization of the active materials. Up to now, the main synthesis method for preparing VN/carbon composites

Received: October 10, 2017
Revised: December 8, 2017
Published: December 8, 2017

DOI: 10.1021/acs.jpcc.7b10021
J. Phys. Chem. C 2018, 122, 143−149

Scheme 1. Schematic Representation for Fabrication Strategy

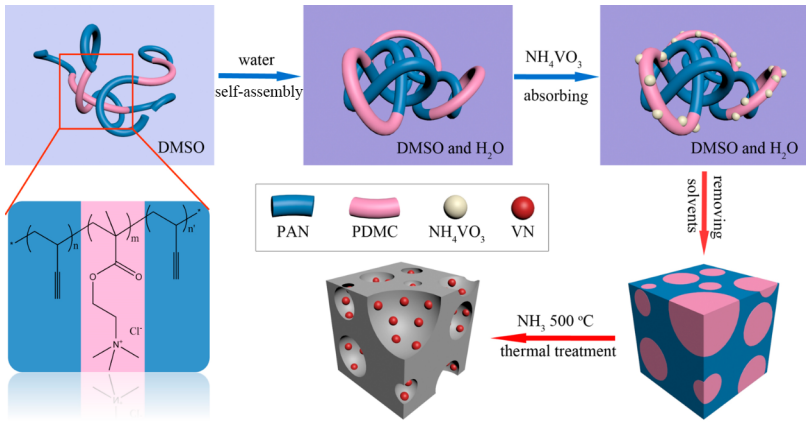

materials is chemical deposition of transition-metal nitrides onto porous carbon materials or simple physical composition. In this article, we found out a valid dispersion method of VN nanoparticles into the surface of porous carbon materials, which was derived from a synthesized block copolymer of polyacrylonitrile-*b*-poly[2-(methacryloyloxy)ethyl]trimethylammonium chloride-*b*-polyacrylonitrile (PAN-*b*-PDMC-*b*-PAN) absorbed with ammonium metavanadate (NH_3VO_3). With the superiority of the designed structure, the fabricated materials were used as negative materials for capacitors electrode and showed outstanding electrochemical performance. In addition, the effect of the ratio of copolymer to NH_3VO_3 on the electrochemical performance of the product was also investigated in detail.

2. EXPERIMENTAL SECTION

2.1. Chemicals. [2-(Methacryloyloxy)ethyl]trimethylammonium chloride (DMC, analytical reagent) and acrylonitrile (AN, analytical reagent) were purchased from Aladdin, and subjected to distillation treatment prior to use. Ammonium metavanadate (NH_4VO_3, analytical reagent), azobisisobutyronitride (AIBN), dimethylformamide (DMF, analytical reagent), and dimethyl sulfoxide (DMSO, analytical reagent) were purchased from Sinopharm Chemical Reagent Co. Ltd., and used as received. The reversible addition−fragmentation chain transfer polymerization (RAFT) agent of trithiocarbonate (BDMAT) was synthesized according to the literature.[37]

2.2. Synthesis of PAN-*b*-PDMC-*b*-PAN. In a typical synthesis, 0.014 g of AIBN (8.5×10^{-5} mol), 0.0282 g of BDMAT (0.001 mol), 4.8 g of AN (0.09 mol), and 5 mL of DMF were mixed together in a 50 mL single-neck round-bottom flask at room temperature under magnetic stirring in a nitrogen atmosphere. The mixture was then degassed by a four freeze−pump−thaw cycle in order to get rid of oxygen, and then heated to 70 °C in a nitrogen atmosphere where polymerization took place for 7 h. After the reaction, the resulting polyacrylonitrile (PAN) was precipitated by methyl alcohol with water, and dried at 60 °C under vacuum for 12 h. For copolymerization of AN, and DMC, the prepared PAN was further used as macro-RAFT agent. Typically, PAN (1 g), AIBN (4 mg, 2.44×10^{-5} mol), and a specific amount of DMC were mixed into 25 mL of DMF, which was heated in a water bath and reacted at 75 °C in a nitrogen atmosphere for 12 h. The block polymer PAN-*b*-PDMC-*b*-PAN was obtained by being precipitated in ether and dried at 60 °C under vacuum for 48 h.

2.3. Loading Vanadium-Containing Group on Polymer Micelles. Polymer micelles was prepared by dissolving 0.2 g of block polymer PAN-*b*-PDMC-*b*-PAN obtained above into 18 mL of DMSO under a magnetic stirring, into which 6 mL of H_2O was dropwise added in half an hour. The mixture was then stirred for another half an hour in order to form a uniform micellar solution and promote the cross-linking of block copolymer. After that, excessive NH_4VO_3 was added under natural light while maintaining stirring, and the loading reaction was carried out for another 72 h.

2.4. Preparation of Carbon and Vanadium Nitride Composite Materials (VN/C). The polymer micelle/NH_4VO_3 system was centrifuged to get the purple colloidal in the interlayer, which was heated in an oven at 30 °C for 24 h and taken a preoxidation at 250 °C under air flow for 6 h; after being cooled down, a thermal treatment was carried out at 800 °C in a tube furnace under a N_2/NH_3 gas mixture (40/100 sccm) atmosphere for 1 h at a temperature ramp of 5 °C/min. The obtained product of VN/C was preserved in rotary dryer for use.

2.5. Materials Characterization. The microstructures and morphology were examined by scanning electron microscopy (SEM, Hitachi S-4800) and transition electron microscopy (TEM, JEOL JEM2010) measurements. The crystal structure was analyzed by X-ray diffraction (XRD Bruker, D8 Advance, Germany). X-ray photoelectron spectroscopy (XPS) (V.G. ESCA Laboratory 210) was used as characterization method of composite components reflecting the composite distribution of microstructural components. The VN contents in composite materials were measured by using a thermo gravimetric analyzer (TGA) and differential thermal analysis (DTA) tests.

2.6. Electrochemical Measurements. Three-electrode cells were assembled to measure the electrochemical properties of the materials. To prepare a working electrode, carbon/VN (80 wt %), carbon black (5 wt %), acetylene black (5 wt %), and polytetrafluoroethylene (10 wt %) were mixed to make a homogeneous black paste. The resulting slurry was spread onto a piece of nickel foam, which served as a current collector. The nickel foam was heated at 60 °C for 10 h in air. Each electrode contained 4 mg of electro-active material and had a geometric surface area of about 1 cm^2.

Electrochemical performances, i.e., cycle voltammetry, galvanostatic charging/discharging measurements, and electrical impedance spectroscopy, were carried out by using a CHI660E (Shanghai, China) in a three-electrode system in 2 M KOH aqueous electrolyte at room temperature. A platinum

DOI: 10.1021/acs.jpcc.7b10021
J. Phys. Chem. C 2018, 122, 143−149

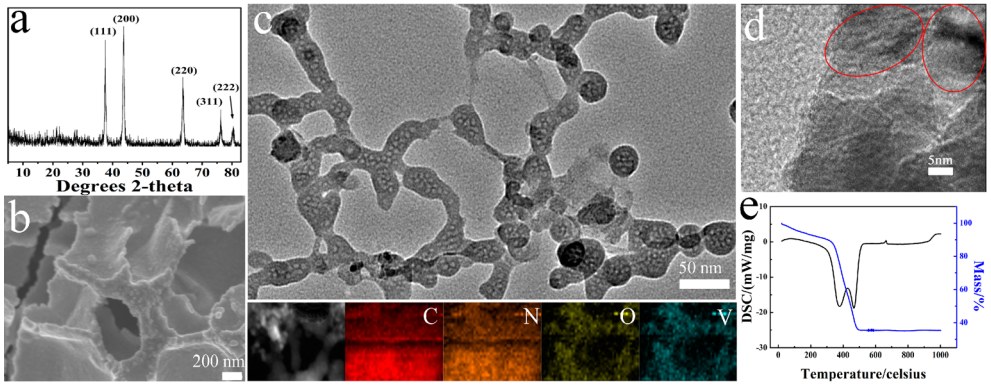

Figure 1. (a) XRD pattern, (b) SEM, (c and d) TEM, and (e) TGA (axis on left) and DTA (axis on right) analysis of VN/C.

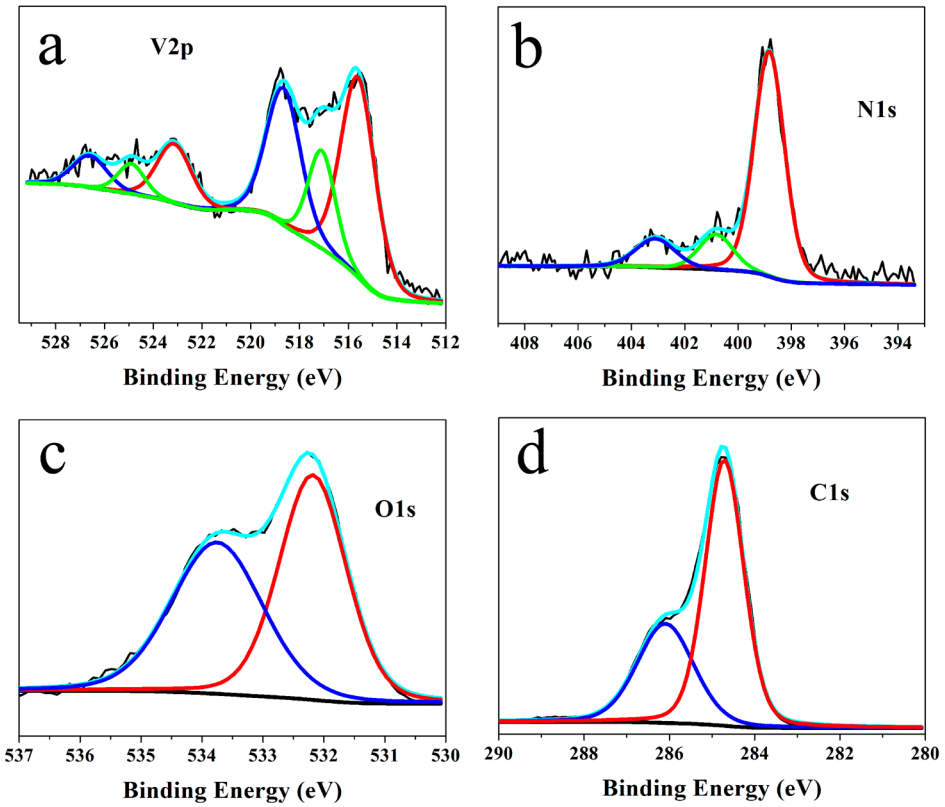

Figure 2. XPS data of (a) V $2p^3$, (b) N 1s, (c) O 1s, and (d) C 1s for VN/C.

gauze electrode served as the counter electrode, and a saturated calomel electrode served as the reference electrode. Cycle-life test for the symmetric cell used a battery test system (Land CT2001A model). The specific capacitance (C) was calculated by the following equation

$$C = I/[(\mathrm{d}E/\mathrm{d}t)m] = I/[(\Delta E/\Delta t) \times m]\ (\mathrm{F/g}) \qquad (1)$$

where I, Δt, m, and ΔE are constant discharging current, the time period for a full discharging, the mass of the corresponding active electrode material, and the electrode potential change after a full discharging, respectively.

3. RESULTS AND DISCUSSION

The block copolymer of PAN-*b*-PDMC-*b*-PAN was synthesized by RAFT polymerization, and the detailed process is provided in the Experimental Section. The fabrication procedure of carbon/vanadium nitrides (C/VN) nanocomposites could be illustrated as Scheme 1. In the first step, the block copolymer of PAN-*b*-PDMC-*b*-PAN was put into DMSO to get stretching polymer chains. Then, H_2O was dropped into the solution to make the polymer chains be self-assembled: hydrophobic segments of −PAN shrank and intertwined with each other; at the same time, the hydrophilic segments of −PDMC kept stretching. In this process, the self-assembled micelles decided the final product feature: −PAN block formed the carbon skeleton, and −PDMC chains were sacrificed, leaving the cellular structure. Second, after adding NH_4VO_3 powder into the solution, the formed VO_3^- ions can be trapped by −PDMC chains in the aqueous environment. This process effectively made the product of VN combined on the surface of the carbon skeleton, so as to achieve good electronic transmission efficiency. Third, the polymer micelle/NH_4VO_3 system was centrifuged to get the purple colloidal in the interlayer and remove the excess NH_4VO_3 and solvents to guarantee saturated

DOI: 10.1021/acs.jpcc.7b10021
J. Phys. Chem. C 2018, 122, 143−149

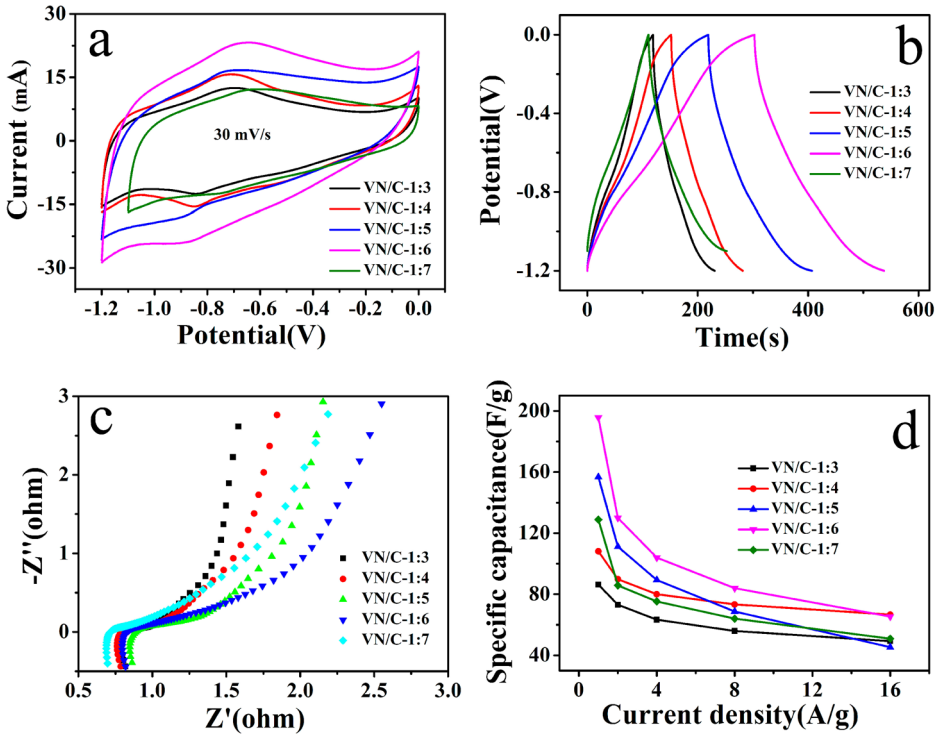

Figure 3. Electrochemical properties of VN/C in 2 M KOH electrolyte: (a) CV curves at the rate of 30 mV/s, (b) charging/discharging curves, (c) Nyquist plots, and (d) capacitance retention at various current densities.

loading of the VO_3^- on −PDMC chains. Finally, the colloidal was heat-treated at ammonia to get the VN/C nanocomposites. The fabricated VN/Cs with the various polymer/NH_4VO_3 ratios of 1:3, 1:4, 1:5, 1:6, and 1:7 were named as VN/C-1:3, VN/C-1:4, VN/C-1:5, VN/C-1:6, and VN/C-1:7.

The prepared VN/C nanocomposites were characterized, and the results are shown in Figure 1. The XRD pattern was identical to the PDF file of 35-0768, which presented the cubic VN and the Bragg peaks indexed to the diffractions of (111), (200), (220), (311), and (222) (Figure 1a). This can be demonstrated that VO_3^- ions were caught by −PDMC and have successfully converted into VN. The background bump before 30° was the characteristic peak of carbon, and these of sharp little peaks were the evidence of the admixture of vanadium oxide and vanadium nitride, which can be further proved by the XPS data. Our designed structure can be clearly seen from the SEM images (Figure 1b), which showed a connected carbon skeleton with a rich pore structure. Thanks to the sacrificed part of hydrophilic chains in the block copolymers, there were lots of micropores in the carbon skeleton (Figure 1c). These hierarchical porosity structures not only released the compound body mass but also provided the ion buffer pool for the quick charge transfer from/to the electrolyte. Meanwhile, the connected carbon skeleton with the rich pore structure made the specific surface of the material be fully utilized during the electrochemical process. In the elements mapping images, one can find that vanadium distributed into the carbon skeleton surface, and there was partial oxidation on the surface of VN. The distribution of nitrogen was the same as carbon, which was caused by nitride doping of carbon source derived from −PAN chains. From the HRTEM pattern (Figure 1d), one can find the definite boundary of the carbon skeleton and VN-involved layer. In the VN layer, there were some quantum sized dots with the size of about 5−10 nm, which were surrounded by an amorphous structure carbon. This "carbon shell" was good for the VN dots to keep its shape and helped enhance the electrochemical cycle life.[38] TGA and DSC were further tested in air condition, and the calculated mass ratio of VN to carbon was 25/75 (wt/wt) (Figure 1e). Before 300 °C, the cavern trend was caused by the decomposition of oxygen-containing (include the bound water) and nitrogenous groups.[39] Followed by this, a dramatic loss took place owing to the combustion of carbon into CO_2. However, in the DSC curve, the line displayed an obvious fluctuation because of the transformation of VN into V∼N∼O and finally to V_2O_5.[40]

Figure 2 provides the XPS data performed to accurately get the element valences and bonding details. V $2p^1$ and V $2p^3$ appeared to be a sum of the special lines from several valence states of vanadium (Figure 2a). The binding energies for V^{3+}, V^{4+}, and V^{5+} species were three Gaussian distributions with a statistical deviation of W_{BE} = 0.25 eV centered at 515.6, 516.5, and 517.3 eV, respectively. In this point, it means a probability of 70% binding energy was in the reported range of $\delta \pm 0.25$ and a probability of 90% within the range of $\delta \pm 0.5$.[40,41] In Figure 2b, the binding energy of 398.2 eV was associated with the value for VN,[42] and the binding energy of 400.8 eV is for the pyrrolic (N-5) bond.[43] This was caused by the heat treatment under an ammonia atmosphere and the nitrogen-rich carbon source from −PAN chains. In addition, the characteristic peak at 403.3 eV corresponded to N∼O formed in the surface of the oxide layer of vanadium nitride. In the O 1s spectrum in Figure 2c, the characteristic peak was fitted into two main peaks at 532.2 and 533.8 eV also due to the surface oxidation of vanadium nitride. The peak at 532.2 eV was mainly from vanadium oxide and the other one was from the V∼N∼O.[43] The peak of C 1s was easily to be distinguished that the 284.8 eV was typically fitted for the highly oriented

DOI: 10.1021/acs.jpcc.7b10021
J. Phys. Chem. C 2018, 122, 143−149

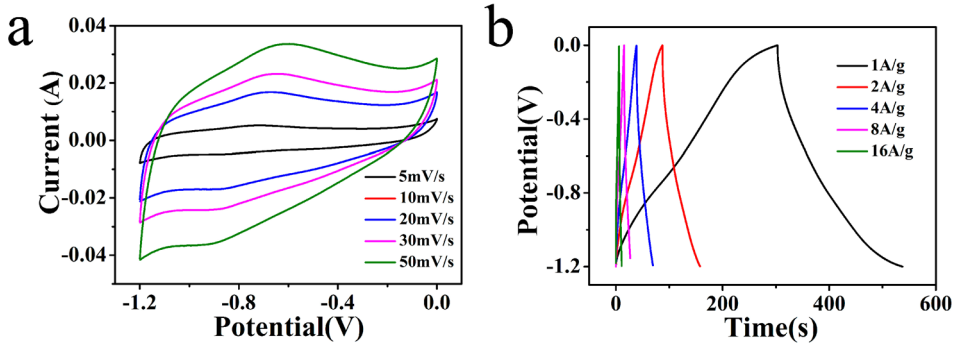

Figure 4. Electrochemical properties of VN/C-1:6 in 2 M KOH electrolyte: (a) CV curves at various scan rates (5−50 mV/s), and (b) charging/discharging curves at various current densities.

pyrolytic graphite (HOPG), and the 286.3 eV was echoed to the nitrogen in the pyrrolic (N-5) bond (Figure 2d).

A three-electrode system in 2 M KOH electrolyte with a Hg/Hg_2Cl_2 reference electrode and a Pt counter-electrode was used to investigate the electrochemical performance of the product. The working electrode was prepared by pressing together the active-material powder and conductive additives into Ni foam. In Figure 3a, the CV curves showed approximately a rectangular mirror image at the scan rate of 30 mV/s, reflecting an ideal capacitive behavior and fast charging propagations within the electrodes. Also, most of the CV curves had a potential window of 1.2 V, except the sample of VN/C-1:7. This result accorded with our original design that, with the different ratio of the sacrificed chain in the block copolymer, there will be two extreme phenomena. If the ratio was low, the VN content in the final material was also low (Figure S1a). However, if the ratio was too high, the specific capacitance did not grow anymore. This was because the sacrifice chains were in the middle of the block copolymer, and too long of the sacrifice chains led to a too thin carbon skeleton, which even broke (Figure S1b). In this case, the vanadium-containing groups would fall down. Meanwhile, a pair of peaks were observed in the CV curves for all the samples, indicating that the oxidation of the VN surface led to a reversible redox reaction of vanadium. The distinguishable redox peak was nearly from −0.84 to −0.57eV; in this area, vanadium underwent a redox reaction that spans the II and III ionization states in a strong alkali environment.[44−46] The sweep-rate dependence of the response current is drawn in Figure 3b to further identify the fact described above. It has the same tendency with the CV curves that the specific capacitance offered upgraded first then descended. The shapes of the galvanostatic charging−discharging curves of VN/C-1:7 coincided with that of the VN/C-1:3. The carbon mass of all the materials was the same, while that of VN was different. After calculation with the galvanostatic charging−discharging curves, the specific capacitances of VN/C-1:3, VN/C-1:4, VN/C-1:5, VN/C-1:6, and VN/C-1:7 were 93.3, 108.2, 156.8, 195.7, and 128.3 F/g. For VN/C-1:7, the contribution of the specific capacitance by VN in the composite was estimated up to 782.8 F/g. EIS measurements were further employed to study the electrochemical impedance of the prepared electrode materials. As shown in Figure 3c, all the samples almost had the same intrinsic impedance, except for VN/C-1:7 due to the highest carbon content. Figure 3d shows the capacitance retentions at various currents. Even though all the samples still presented good properties at high current density, however, the specific capacitance of the pure VN materials without any carbon content displayed only about 70 F/g, which was lower than those of the above composites (Figure S2a,b).

The detailed electrochemical performance of VN/C-1:6 in the 2 M KOH is shown in Figure 4. The cyclic voltammetry curves were rectangular-like at a relatively low scan rate and retained the shape with the scan rate reaching up to 50 mV/s (Figure 4a). This is because the connected structure of the carbon skeleton and the appropriate content of VN made the charging transfer fast and interfacial reaction sufficient. The galvanostatic charging−discharging test performed at different current densities is shown in Figure 4b. The good symmetrical characteristic of charging/discharging curves further revealed that this compound material had excellent electrochemical capability and electrochemical reversibility. Also, there was no platform, indicating that the prepared material was a kind of capacitive material.

The fabricated material of VN/C had the unique structure, which involved the carbon skeleton that served as abundant ion buffer pools that made the charging and discharging process quick and sufficient, and well-dispersed VN nanoparticles on the surface of porous carbon that made the active materials effective. In this way, the material of VN/C had a good cycling stability with high capacitance retention of 75% and nearly 100% Coulombic efficiency after 5000 cycles, as shown in Figure 5.

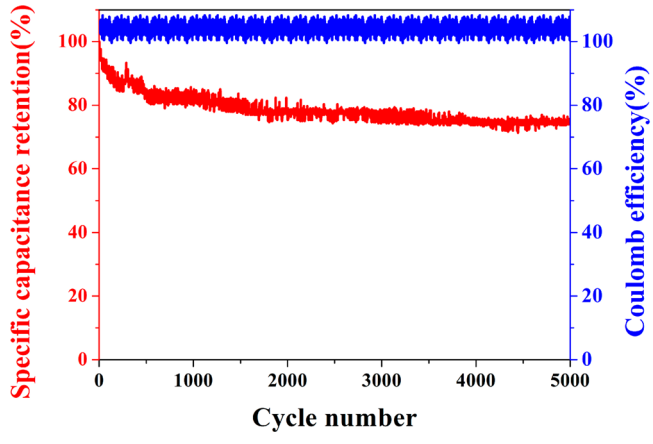

Figure 5. VN/C-1:6 in 2 M KOH electrolyte cycling life at the current density of 5 A/g.

DOI: 10.1021/acs.jpcc.7b10021
J. Phys. Chem. C 2018, 122, 143−149

4. CONCLUSIONS

In summary, we reported a kind of preparation approach to gain the nanohybrid material of vanadium nitride/carbon by using the block copolymer of PAN-*b*-PDMC-*b*-PAN as precursor. With the unique structure of vanadium nitride nanoparticles dispersed in the surface of porous carbon, the fabricated material showed outstanding electrochemical performance with the high specific capacitance of 195.7 F/g. Also, a good cycling stability with a capacitance retention of 75% and nearly 100% Coulombic efficiency after 5000 cycles were obtained.

■ ASSOCIATED CONTENT

Supporting Information

The Supporting Information is available free of charge on the ACS Publications website at DOI: 10.1021/acs.jpcc.7b10021.

Electrochemical properties including CV, GCD curves, and Nyquist plot of pure VN in 2 M KOH electrolyte; SEM images for the samples of VN/C-1:3 and VN/C-1:7 (PDF)

■ AUTHOR INFORMATION

Corresponding Author

*E-mail: ranfen@163.com, ranfen@lut.cn.

ORCID

Lingbin Kong: 0000-0002-2271-4202

Fen Ran: 0000-0002-7383-1265

Notes

The authors declare no competing financial interest.

■ ACKNOWLEDGMENTS

This work was partly supported by the National Natural Science Foundation of China (51203071, 51363014, 51463012, and 51763014), the China Postdoctoral Science Foundation (2014M552509, and 2015T81064), Natural Science Funds of the Gansu Province (1506RJZA098), and the Program for Hongliu Distinguished Young Scholars in Lanzhou University of Technology (J201402).

■ REFERENCES

(1) Xu, J.; Gu, P.; Zhang, J.; Xue, H.; Pang, H. Copper-Based Nanomaterials for High-Performance Lithium-Ion Batteries. *Part. Part. Syst. Char.* **2016**, *33*, 784−810.

(2) Zheng, S.; Xue, H.; Pang, H. Supercapacitors Based on Metal Coordination Materials. *Coord. Chem. Rev.* **2017**.

(3) Thackeray, M. M.; Wolverton, C.; Isaacs, E. D. Electrical Energy Storage for Transportation—Approaching the Limits of, and Going Beyond, Lithium-Ion Batteries. *Energy Environ. Sci.* **2012**, *5*, 7854−7863.

(4) Chalk, S. G.; Miller, J. F. Key Challenges and Recent Progress in Batteries, Fuel Cells, and Hydrogen Storage for Clean Energy Systems. *J. Power Sources* **2006**, *159*, 73−80.

(5) Zhang, Q.; Uchaker, E.; Candelaria, S. L.; Cao, G. Nanomaterials for Energy Conversion and Storage. *Chem. Soc. Rev.* **2013**, *42*, 3127−3171.

(6) Whittingham, M. S. Materials Challenges Facing Electrical Energy Storage. *MRS Bull.* **2008**, *33*, 411−419.

(7) Shukla, A. K.; Banerjee, A.; Ravikumar, M. K.; Jalajakshi, A. Electrochemical Capacitors: Technical Challenges and Prognosis for Future Markets. *Electrochim. Acta* **2012**, *84*, 165−173.

(8) Choi, N. S.; Chen, Z.; Freunberger, S. A.; Ji, X.; Sun, Y. K.; Amine, K.; Yushin, G.; Nazar, L. F.; Cho, J.; Bruce, P. G. Challenges Facing Lithium Batteries and Electrical Double-Layer Capacitors. *Angew. Chem., Int. Ed.* **2012**, *51*, 9994−10024.

(9) Wang, G.; Zhang, L.; Zhang, J. A Review of Electrode Materials for Electrochemical Supercapacitors. *Chem. Soc. Rev.* **2012**, *41*, 797−828.

(10) Landi, B. J.; Ganter, M. J.; Cress, C. D.; Dileo, R. A.; Raffaelle, R. P. Carbon Nanotubes for Lithium Ion Batteries. *Energy Environ. Sci.* **2009**, *2*, 638−654.

(11) Goodenough, J. B.; Kim, Y. Challenges for Rechargeable Li Batteries. *Chem. Mater.* **2010**, *22*, 587−603.

(12) Zhang, F.; Zhang, T.; Yang, X.; Zhang, L.; Leng, K.; Huang, Y.; Chen, Y. A High-Performance Supercapacitor-Battery Hybrid Energy Storage Device Based on Graphene-Enhanced Electrode Materials with Ultrahigh Energy Density. *Energy Environ. Sci.* **2013**, *6*, 1623−1632.

(13) Kim, H. S.; Cook, J. B.; Lin, H.; Ko, J. S.; Tolbert, S. H.; Ozolins, V.; Dunn, B. Oxygen Vacancies Enhance Pseudocapacitive Charge Storage Properties of MoO_{3-x}. *Nat. Mater.* **2017**, *16*, 454−460.

(14) Nitta, N.; Yushin, G. High-Capacity Anode Materials for Lithium-Ion Batteries: Choice of Elements and Structures for Active Particles. *Part. Part. Syst. Char.* **2014**, *31*, 317−336.

(15) Osiak, M.; Geaney, H.; Armstrong, E.; O'Dwyer, C. Structuring Materials for Lithium-Ion Batteries: Advancements in Nanomaterial Structure, Composition, and Defined Assembly on Cell Performance. *J. Mater. Chem. A* **2014**, *2*, 9433−9460.

(16) Kang, B.; Ceder, G. Battery Materials for Ultrafast Charging and Discharging. *Nature* **2009**, *458*, 190−193.

(17) Lai, X.; Halpert, J. E.; Wang, D. Recent Advances in Micro-/Nano-Structured Hollow Spheres for Energy Applications: From Simple to Complex Systems. *Energy Environ. Sci.* **2012**, *5*, 5604−5618.

(18) Sharma, P.; Bhatti, T. S. A Review on Electrochemical Double-Layer Capacitors. *Energy Convers. Manage.* **2010**, *51*, 2901−2912.

(19) MacFarlane, D. R.; Tachikawa, N.; Forsyth, M.; Pringle, J. M.; Howlett, P. C.; Elliott, G. D.; Davis, J. H., Jr; Watanabe, M.; Simon, P.; Angell, C. A. Energy Applications of Ionic Liquids. *Energy Environ. Sci.* **2014**, *7*, 232−250.

(20) Fraser, K. J.; MacFarlane, D. R. Phosphonium-Based Ionic Liquids: An Overview. *Aust. J. Chem.* **2009**, *62*, 309−321.

(21) Lu, Y.; Li, B.; Zheng, S.; Xu, Y.; Xue, H.; Pang, H. Syntheses and Energy Storage Applications of M_xS_y (M = Cu, Ag, Au) and Their Composites: Rechargeable Batteries and Supercapacitors. *Adv. Funct. Mater.* **2017**, *27*, 1703949.

(22) Zheng, S.; Li, X.; Yan, B.; Hu, Q.; Xu, Y.; Xiao, X.; Xue, H.; Pang, H. Transition-Metal (Fe, Co, Ni) Based Metal-Organic Frameworks for Electrochemical Energy Storage. *Adv. Energy Mater.* **2017**, *7*, 1602733.

(23) Li, B.; Zhang, G.; Huang, K.; Qiao, L.; Pang, H. One-Step Synthesis of $CoSn(OH)_6$ Nanocubes for High-Performance All Solid-State Flexible Supercapacitors. *Rare Met.* **2017**, *36*, 457−464.

(24) Liu, L.; Shen, B.; Jiang, D.; Guo, R.; Kong, L.; Yan, X. Watchband-Like Supercapacitors with Body Temperature Inducible Shape Memory Ability. *Adv. Energy Mater.* **2016**, *6*, 1600763.

(25) Yu, M.; Zeng, Y.; Han, Y.; Cheng, X.; Zhao, W.; Liang, C.; Tong, Y.; Tang, H.; Lu, X. Valence-Optimized Vanadium Oxide Supercapacitor Electrodes Exhibit Ultrahigh Capacitance and Super-Long Cyclic Durability of 100 000 Cycles. *Adv. Funct. Mater.* **2015**, *25*, 3534−3540.

(26) Tang, H.; Wang, J.; Yin, H.; Zhao, H.; Wang, D.; Tang, Z. Growth of Polypyrrole Ultrathin Films on MoS_2 Monolayers as High-Performance Supercapacitor Electrodes. *Adv. Mater.* **2015**, *27*, 1117−1123.

(27) Wang, Q.; Yan, J.; Fan, Z. Carbon Materials for High Volumetric Performance Supercapacitors: Design, Progress, Challenges and Opportunities. *Energy Environ. Sci.* **2016**, *9*, 729−762.

(28) Lin, T.; Chen, I.; Liu, F.; Yang, C.; Bi, H.; Xu, F.; Huang, F. Nitrogen-Doped Mesoporous Carbon of Extraordinary Capacitance for Electrochemical Energy Storage. *Science* **2015**, *350*, 1508−1513.

(29) Wang, G.; Wang, H.; Lu, X.; Ling, Y.; Yu, M.; Zhai, T.; Tong, Y.; Li, Y. Solid-State Supercapacitor Based on Activated Carbon Cloths Exhibits Excellent Rate Capability. *Adv. Mater.* **2014**, *26*, 2676−2682.
(30) Chen, T.; Dai, L. Carbon Nanomaterials for High-Performance Supercapacitors. *Mater. Today* **2013**, *16*, 272−280.
(31) Li, X.; Ding, S.; Xiao, X.; Shao, J.; Wei, J.; Pang, H.; Yu, Y. N. S Co-Doped 3D Mesoporous Carbon−$Co_3Si_2O_5(OH)_4$ Architectures for High-Performance Flexible Pseudo-Solid-State Supercapacitors. *J. Mater. Chem. A* **2017**, *5*, 12774−12781.
(32) Lu, X.; Yu, M.; Zhai, T.; Wang, G.; Xie, S.; Liu, T.; Liang, C.; Tong, Y.; Li, Y. High Energy Density Asymmetric Quasi-Solid-State Supercapacitor Based on Porous Vanadium Nitride Nanowire Anode. *Nano Lett.* **2013**, *13*, 2628−2633.
(33) Bondarchuk, O.; Morel, A.; Bélanger, D.; Goikolea, E.; Brousse, T.; Mysyk, R. Thin Films of Pure Vanadium Nitride: Evidence for Anomalous Non-Faradaic Capacitance. *J. Power Sources* **2016**, *324*, 439−446.
(34) Zhang, Q.; Wang, X.; Pan, Z.; Sun, J.; Zhao, J.; Zhang, J.; Zhang, C.; Tang, L.; Luo, J.; Song, B.; et al. Wrapping Aligned Carbon Nanotube Composite Sheets around Vanadium Nitride Nanowire Arrays for Asymmetric Coaxial Fiber-Shaped Supercapacitors with Ultrahigh Energy Density. *Nano Lett.* **2017**, *17*, 2719−2726.
(35) Lee, H. M.; Jeong, G. H.; Kim, S. W.; Kim, C. K. Low-Temperature Direct Synthesis of Mesoporous Vanadium Nitrides for Electrochemical Capacitors. *Appl. Surf. Sci.* **2017**, *400*, 194−199.
(36) Vijayakumar, P.; Senthil Pandian, M.; Pandikumar, A.; Ramasamy, P. Electrochemical Interfacial Charge Transfer Dynamics and Photovoltaic Performances of Nanofibrous Vanadium Derivatives Based Platinum Free Counter Electrodes in Dye Sensitized Solar Cells. *Mater. Sci. Eng., B* **2017**, *222*, 7−17.
(37) Lai, J. T.; Filla, D.; Shea, R. Functional Polymers from Novel Carboxyl-Terminated Trithiocarbonates as Highly Efficient RAFT Agents. *Macromolecules* **2002**, *35*, 6754−6756.
(38) Lu, X.; Liu, T.; Zhai, T.; Wang, G.; Yu, M.; Xie, S.; Ling, Y.; Liang, C.; Tong, Y.; Li, Y. Improving the Cycling Stability of Metal−Nitride Supercapacitor Electrodes with a Thin Carbon Shell. *Adv. Energy Mater.* **2014**, *4*, 1300994.
(39) McAllister, M. J.; Li, J. L.; Adamson, D. H.; Schniepp, H. C.; Abdala, A. A.; Liu, J.; Herrera-Alonso, M.; Milius, D. L.; Car, R.; Prud'homme, R. K.; et al. Single Sheet Functionalized Graphene by Oxidation and Thermal Expansion of Graphite. *Chem. Mater.* **2007**, *19*, 4396−4404.
(40) Biedunkiewicz, A.; Gabriel, U.; Figiel, P.; Sabara, M. Investigations on NH_4VO_3 Thermal Decomposition in Dry Air. *J. Therm. Anal. Calorim.* **2012**, *108*, 965−970.
(41) Bondarenka, V.; Grebinskij, S.; Mickevicius, S.; Tvardauskas, H.; Kaciulis, S.; Volkov, V.; Zakharova, G.; Pašiškevicius, A. Valence of Vanadium in Hydrated Compounds. *Lith. J. Phys.* **2007**, *47*, 333−342.
(42) Choi, D.; Blomgren, G. E.; Kumta, P. N. Fast and Reversible Surface Redox Reaction in Nanocrystalline Vanadium Nitride Supercapacitors. *Adv. Mater.* **2006**, *18*, 1178−1182.
(43) Zhang, L.; Holt, C. M. B.; Luber, E. J.; Olsen, B. C.; Wang, H.; Danaie, M.; Cui, X.; Tan, X.; Lui, V. W.; Kalisvaart, W. P.; Mitlin, D. High Rate Electrochemical Capacitors from Three-Dimensional Arrays of Vanadium Nitride Functionalized Carbon Nanotubes. *J. Phys. Chem. C* **2011**, *115*, 24381−24393.
(44) Al-Kharafi, F. M.; Badawy, W. A. Electrochemical Behaviour of Vanadium in Aqueous Solutions of Different pH. *Electrochim. Acta* **1997**, *42*, 579−586.
(45) Kelsall, G. H.; Thompson, I.; Francis, P. A. Redox Chemistry of H_2S Oxidation by the British Gas Stretford Process Part IV: V-S-H_2O Thermodynamics and Aqueous Vanadium (v) Reduction in Alkaline Solutions. *J. Appl. Electrochem.* **1993**, *23*, 417−426.
(46) Yan, Y.; Li, B.; Guo, W.; Pang, H.; Xue, H. Vanadium Based Materials as Electrode Materials for High Performance Supercapacitors. *J. Power Sources* **2016**, *329*, 148−169.

DOI: 10.1021/acs.jpcc.7b10021
J. Phys. Chem. C 2018, 122, 143−149